Stochastic coupled mode theory for partially coherent laser arrays

Dominic F. Siriani,* Kent D. Choquette, and P. Scott Carney

Department of Electrical and Computer Engineering, University of Illinois, Urbana, Illinois 61801, USA
*Corresponding author: siriani@illinois.edu

Partially coherent, transversely coupled laser arrays are investigated within a stochastic coupled mode formalism. Predictions of the coherence or correlation functions in both the spectral and time domains are made. It is demonstrated that the coherence properties of the system in both domains are strongly dependent on the number and intensity of coupled modes. The theory can be useful for the study of semiconductor laser arrays, particularly vertical-cavity surface-emitting laser arrays. © 2010 Optical Society of America

OCIS codes: 030.1640, 140.2010, 140.7260, 230.4555.

1. INTRODUCTION

Semiconductor laser arrays are of interest for applications in communications, sensing, and various other optical applications. Vertical-cavity surface-emitting laser (VCSEL) arrays are of special consequence because of the ease of two-dimensional array fabrication [1–3]. Recent progress with VCSEL arrays has demonstrated their potential for increased-power, low-diffraction, single-mode laser sources and electrically controllable laser steering in two dimensions [4,5]. These laser arrays have been shown to couple via both evanescent [6–8] and leaky [9,10] fields. The focus of this work is the former coupling mechanism.

To analyze semiconductor laser arrays, a variety of approaches have been taken based on the manner of the coupling [11–13]. For evanescently coupled lasers, coupled mode theory has been a valuable tool and has successfully predicted the observed spatial modes [14,15]. However, VCSEL arrays have demonstrated partially coherent behavior that is not explained within the deterministic coupled mode theory [16]. To address this issue, a stochastic harmonic oscillator model was recently developed [17]. Although this model well describes partially coherent arrays, it is unable to predict, *ab initio*, the spectra and coupling strength.

A stochastic coupled mode formalism is developed below. The coherence matrices in the time and frequency domains are derived. The stochastic model is compared with deterministic coupled mode theory. This new model predicts the observed partially coherent operation of the array as well as the spectra and coupling strength obtained from deterministic coupled mode theory.

2. COUPLED MODE FORMALISM

In this work, laser arrays are modeled as coupled waveguides terminated by the top and bottom reflectors, forming simple Fabry–Perot cavities. A schematic representation of the problem under investigation is shown in Fig. 1. This formulation is applicable to a wide variety of devices such as VCSEL arrays, edge-emitting laser arrays, and laser amplifier arrays. For VCSELs, an effective mirror model can be used to reduce the structure to the one investigated here [18].

Following the analysis given in [19], the field solutions for two coupled waveguides, a and b, are given by

$$U(x,y,z) = a(z)U^{(a)}(x,y) + b(z)U^{(b)}(x,y), \qquad (1)$$

where $U^{(a)}$ and $U^{(b)}$ are the unperturbed transverse mode profiles of the waveguides with complex propagation constants β_a and β_b, respectively, and all quantities should be understood to depend on frequency. In [20], an approximate theory of coupled Fabry–Perot devices is derived, giving the transmitted field at the output mirror located at $z=z_0$:

$$\begin{bmatrix} a(z_0) \\ b(z_0) \end{bmatrix} = \mathbf{VFV}^{-1} \begin{bmatrix} a(0) \\ b(0) \end{bmatrix}, \qquad (2)$$

where

$$\mathbf{V} = \begin{bmatrix} K & K \\ \Delta\beta + \psi & \Delta\beta - \psi \end{bmatrix}, \qquad (3)$$

$$\mathbf{F} = \begin{bmatrix} \xi_+(\omega) & 0 \\ 0 & \xi_-(\omega) \end{bmatrix}. \qquad (4)$$

The terms used here are given in Table 1 and all have dimensions of inverse length.

The diagonal terms of $\mathbf{F}$ are the responses of the Fabry–Perot cavity for the propagation constants, β_+ and β_-, of the $+$ and $-$ mode solutions of the coupled eigenvalue problem. The model does not account for effects of gain saturation, mode competition, gain clamping, etc. Assuming that these effects manifest themselves simply as changes in the overall spectral intensities of the two coupled modes, we arrive at the expressions for a cavity of length L with mirrors of amplitude reflectivity $R_1=R_2=R$:
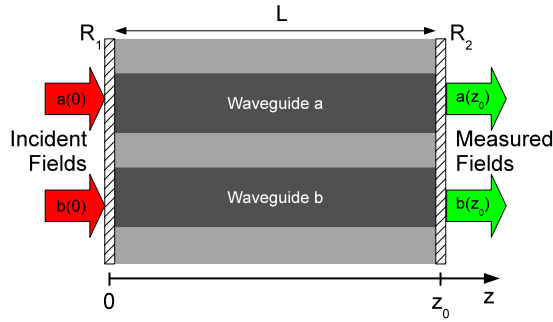
Fig. 1.   (Color online) Sketch of the laser array system under investigation.

$$\xi_+(\omega) = \sigma_+ \frac{(1-R^2)e^{-i\beta_+ L}}{1 - R^2 e^{-i2\beta_+ L}},$$

$$\xi_-(\omega) = \sigma_- \frac{(1-R^2)e^{-i\beta_- L}}{1 - R^2 e^{-i2\beta_- L}}. \tag{5}$$

It also is assumed that the propagation constants and coupling constant vary linearly with frequency:

$$\beta_p = \frac{\omega}{c} n_p, \tag{6}$$

$$K = \frac{\omega}{c} \kappa, \tag{7}$$

where the subscript p is a, b, $+$, or $-$, n_p is the frequency-independent effective refractive index, κ is a unitless coupling term, and c is the vacuum speed of light. The first restriction put on the propagation constants assumes that the waveguides are operating in a linear regime of the dispersion curve. Additionally, in general, κ is frequency dependent, but it is assumed that, over the narrow frequency range of interest, this dependence is negligible and κ may be assumed to be constant.

In terms of the variables defined in Table 2, the matrix **V** is given by

$$\mathbf{V} = \begin{bmatrix} \kappa & \kappa \\ \Delta n + \eta & \Delta n - \eta \end{bmatrix}, \tag{8}$$

while the matrix **F** remains unchanged. Since the lasers of interest in this work have only a single longitudinal mode, the expressions of Eqs. (5) are simplified to Lorentzians:

$$\xi_+(\omega) = \sigma_+ \frac{\alpha}{\alpha + i(\omega - \omega_+)},$$

$$\xi_-(\omega) = \sigma_- \frac{\alpha}{\alpha + i(\omega - \omega_-)}, \tag{9}$$

where ω_+ and ω_- are the resonances of the two modes and α is the total cavity loss.

The theory presented in the following sections is entirely general and does not depend on the specific form of ξ_+ and ξ_-. These assumptions are made for clarity of pre-

Table 1. Definitions of Terms (units, μm^{-1})

Variable	Value	Definition
$\beta_{a,b}$		Propagation constant in a, b
K		Coupling strength
$\bar{\beta}$	$\dfrac{\beta_b + \beta_a}{2}$	Average propagation constant
$\Delta\beta$	$\dfrac{\beta_b - \beta_a}{2}$	Propagation constant difference
ψ	$[\Delta\beta^2 + |K|^2]^{1/2}$	
$\beta_{\pm}$	$\bar{\beta} \pm \psi$	Propagation constant of $\pm$ mode

Table 2. Definitions of Unitless Terms

Variable	Value	Definition
$n_{a,b}$		Effective index of a, b
κ		Coupling strength
$\bar{n}$	$\dfrac{n_b + n_a}{2}$	Average effective index
Δn	$\dfrac{n_b - n_a}{2}$	Effective index difference
η	$[\Delta n^2 + |\kappa|^2]^{1/2}$	
$n_{\pm}$	$\bar{n} \pm \eta$	Effective index of $\pm$ mode
$\omega_{\pm}$	$\dfrac{N\pi c}{n_{\pm} L}$	Resonance of $\pm$ mode (N integer)

sentation; i.e., an explicit frequency dependence of the propagation constants is necessary for numerical calculations.

3. DETERMINISTIC ANALYSIS

Preliminary to addressing the stochastic problem, it is illustrative to review the deterministic coupled mode problem. Explicitly carrying out the matrix and vector operations of Eq. (2) yields the solution

$$\begin{bmatrix} a(z_0) \\ b(z_0) \end{bmatrix} = \frac{1}{2\eta} \begin{bmatrix} A_a^a a(0) + A_a^b b(0) \\ A_b^a a(0) + A_b^b b(0) \end{bmatrix}, \tag{10}$$

where

$$A_a^a = \xi_+(\omega)(\eta - \Delta n) + \xi_-(\omega)(\eta + \Delta n),$$

$$A_a^b = \xi_+(\omega)\kappa - \xi_-(\omega)\kappa,$$

$$A_b^a = \xi_+(\omega)\kappa^* - \xi_-(\omega)\kappa^*,$$

$$A_b^b = \xi_+(\omega)(\eta + \Delta n) + \xi_-(\omega)(\eta - \Delta n). \tag{11}$$

For comparison to the stochastic case, it is useful to calculate the products of the amplitudes, a and b. For an ergodic, stationary, random field, these products form the cross-spectral density matrix, the diagonal elements being the power spectral densities. The cross-spectral density is simply related by Fourier transform to the time-domain correlation and cross-correlation functions; i.e., the Wiener–Khintchine–Einstein theorem [21–23] applies. In computing the deterministic analogue of the

cross-spectral density, some care must be taken. No simple relationship exists between the products of the co-efficients of the fields in the frequency domain at a single frequency and the products of coefficients of the fields in the time domain. With this caveat, we refer to the matrix of Hermitian products of coefficients as the deterministic cross-spectral density. The deterministic cross-spectral density matrix of the output field is given by

$$\mathbf{W} = \begin{bmatrix} a^*(z_0)a(z_0) & a^*(z_0)b(z_0) \\ b^*(z_0)a(z_0) & b^*(z_0)b(z_0) \end{bmatrix} = \frac{1}{|2\eta|^2} \begin{bmatrix} W_{aa} & W_{ab} \\ W_{ba} & W_{bb} \end{bmatrix}. \tag{12}$$

Solving for the matrix in Eq. (12), it is found that the off-diagonal element is expressible in terms of the diagonal terms, viz.,

$$W_{ab} = [W_{aa}W_{bb}]^{1/2}e^{i\phi}, \tag{13}$$

where ϕ is real, and therefore the magnitude of the spectral degree of coherence, defined as

$$|\mu(\omega)| = \left| \frac{W_{ab}}{[W_{aa}W_{bb}]^{1/2}} \right|, \tag{14}$$

is found to be equal to unity, implying that the fields in the two waveguides are completely coherent with each other as must be expected.

Moreover, the coherent mode decomposition is computed via the eigenvalue problem

$$\mathbf{W}\begin{bmatrix} V_a \\ V_b \end{bmatrix} = \lambda \begin{bmatrix} V_a \\ V_b \end{bmatrix}. \tag{15}$$

There is only one coherent mode with a nonzero eigenvalue, given by

$$\begin{bmatrix} V_a \\ V_b \end{bmatrix} = \frac{1}{2\eta^*} \begin{bmatrix} W_{aa}^{1/2}e^{i\phi} \\ W_{bb}^{1/2} \end{bmatrix} = \frac{1}{2\eta^*} \begin{bmatrix} A_a^a a(0) + A_a^b b(0) \\ A_b^a a(0) + A_b^b b(0) \end{bmatrix}^*, \tag{16}$$

with eigenvalue $(W_{aa}+W_{bb})/|2\eta|^2$, as one would expect for a spectrally fully coherent field. Again, some care must be taken in the comparison here as the deterministic field is not statistically stationary.

4. COUPLED MODES FROM INCOHERENT SOURCES

In order to treat stochastic fields, the boundary conditions are taken to be random, stationary, and ergodic. Moreover, it is supposed that the boundary fields in waveguide a and waveguide b are uncorrelated:

$$\langle a^*(0)a(0) \rangle = S_a^{(0)},$$

$$\langle b^*(0)b(0) \rangle = S_b^{(0)},$$

$$\langle a^*(0)b(0) \rangle = 0. \tag{17}$$

Analogously to the deterministic spectral density matrix in Eq. (12), the modal cross correlation at the output mirror is defined by the matrix

$$\mathbf{W} = \begin{bmatrix} \langle a^*(z_0)a(z_0) \rangle & \langle a^*(z_0)b(z_0) \rangle \\ \langle b^*(z_0)a(z_0) \rangle & \langle b^*(z_0)b(z_0) \rangle \end{bmatrix} = \frac{1}{|2\eta|^2} \begin{bmatrix} W_{aa} & W_{ab} \\ W_{ba} & W_{bb} \end{bmatrix}. \tag{18}$$

In terms of the definitions given in Eqs. (11) and (17), the elements of the cross-correlation matrix are

$$W_{aa} = |A_a^a|^2 S_a^{(0)} + |A_a^b|^2 S_b^{(0)},$$

$$W_{bb} = |A_b^a|^2 S_a^{(0)} + |A_b^b|^2 S_b^{(0)},$$

$$W_{ab} = A_a^{a*}A_b^a S_a^{(0)} + A_a^{b*}A_b^b S_b^{(0)}. \tag{19}$$

Unlike in the deterministic case, the spectral degree of coherence is not necessarily of unit magnitude.

One again can solve for the coherent modes of this cross-correlation matrix, although a general expression is particularly complicated. However, two limiting cases can provide insight: when the two spectral terms (ξ_+ and ξ_-) are equal and when only one spectral term is nonzero. For $\xi_+(\omega) = \xi_-(\omega) = \xi(\omega)$, the coherent modes are given by

$$\begin{bmatrix} V_a \\ V_b \end{bmatrix} = \begin{bmatrix} 1 \\ 0 \end{bmatrix}, \tag{20}$$

$$\begin{bmatrix} V_a \\ V_b \end{bmatrix} = \begin{bmatrix} 0 \\ 1 \end{bmatrix}, \tag{21}$$

with eigenvalues $|\xi(\omega)|^2 S_a^{(0)}$ and $|\xi(\omega)|^2 S_b^{(0)}$, respectively. It can be seen here that there are two coherent modes, the intensity of each localized in one waveguide or the other. Additionally, the magnitude of the spectral degree of coherence, since $W_{ab}=0$, is zero.

In the limit where $\xi_{\mp}(\omega)=0$, there is only one mode with a nonzero eigenvalue,

$$\begin{bmatrix} V_a \\ V_b \end{bmatrix} = \begin{bmatrix} \kappa \\ \Delta n \pm \eta \end{bmatrix}^*, \tag{22}$$

with the eigenvalue $(W_{aa}+W_{bb})/|2\eta|^2$. Respectively, these two modes can be identified as the $+$ and $-$ modes as defined in [19]. Since these two cases represent single-mode states, the magnitude of the complex spectral degree of coherence is unity.

Thus, in these two limiting case, the two extremes of complete coherence and incoherence are observed. For conditions lying between these two limits, partial spectral coherence can be observed as is seen below. Therefore, the stochastic coupled mode formalism is capable of predicting partially coherent behavior that was previously inaccessible through deterministic methods.

As a final note, it is important to point out that the results as obtained in the previous section on the deterministic theory can be recovered by using the stochastic theory. That is, when the random seeding fields of the stochastic theory, $a(0)$ and $b(0)$, are completely mutually coherent, the output is single mode and the component mode amplitudes are the same as the deterministic field amplitudes. Thus, the two theories agree for the calculation of observables dependent on the mutual coherence, such as the interference pattern produced in the far zone. However, with the stochastic theory, the fields are station-

Table 3. Parameters Used for Symmetric Calculation

Variable	Definition	Value	Units
$n_{a,b}$	Effective index of a, b	3.5	
κ	Coupling strength	5×10^{-3}	
α	Cavity loss	1.2×10^{12}	rad/s
L	Cavity length	0.243	μm

ary and ergodic, so it is possible to compute quantities that depend not just on the mutual coherence, but on the degree of coherence, such as the power spectra or the autocorrelation. Thus, the stochastic coupled mode theory is capable of making predictions that are in agreement with previously investigated deterministic approaches as well as ones that are inaccessible to the deterministic approach.

5. NUMERICAL SPECTRAL ANALYSIS OF COUPLED LASERS

The results of the previous sections can best be illustrated through numerical calculations. Two particular cases are treated: symmetric and asymmetric waveguides. Calculations are performed for both deterministic and random boundary conditions to demonstrate the significance of the statistical nature of the fields seeding the coupled system.

A. Symmetric Coupled Guides

The device being modeled here is a two-element VCSEL array. The parameters used for the calculations are presented in Table 3. The VCSELs are assumed to operate at 850 nm (angular frequency of 2.218×10^{15} rad/s) and have a full width at half-maximum linewidth of approximately 0.95 nm (2.4×10^{12} rad/s). This corresponds to VCSELs with cavity loss of about 40 cm^{-1}. This value of loss is larger than a typical value for a VCSEL, but it is used primarily for illustration.

The deterministic boundary conditions are $a(0) = b(0) = 1$, and the random conditions are specified by $\langle a*(0)a(0) \rangle = \langle b*(0)b(0) \rangle = 1$ and $\langle a*(0)b(0) \rangle = 0$. In other words, the sources seeding the two waveguides are of

equal intensity. Figure 2 shows the unperturbed spectra for the two guides when no coupling is present. Note that since the waveguides are symmetric, the spectra for guides a and b are identical.

The spectra for guides a and b, respectively represented by W_{aa} and W_{bb}, with deterministic boundary conditions are shown in Fig. 3. In this plot, it can be seen that the spectra from the two guides are identical. Moreover, it is apparent from the single peak that only one coupled mode is excited, specifically the + mode. The coupling between the guides causes a frequency shift of the modes, which is apparent in Fig. 3 since the peak is at a lower frequency than in Fig. 2. This illustrates that, for the deterministic problem, the boundary conditions entirely determine the mode or admixture of modes that is excited, just as here $a(0) = b(0)$ excites the + mode.

From the analysis of the previous section, it is expected that both coupled modes will turn on with equal intensity when stochastic boundary conditions are used. Figure 3 shows the power spectra for guides a and b in the case that the boundary conditions are random. Again, the spectra from the two guides are identical. However, as a result of the stochastic boundary conditions, now both the + and − modes are excited. Thus, unlike the deterministic case, the random boundary conditions equally excite

(a)

(b)

Fig. 3.   (Color online) (a) Deterministic and (b) stochastic coupled power spectra for no detuning between the propagation constants of guides a and b. The spectra from the two guides exactly overlap.

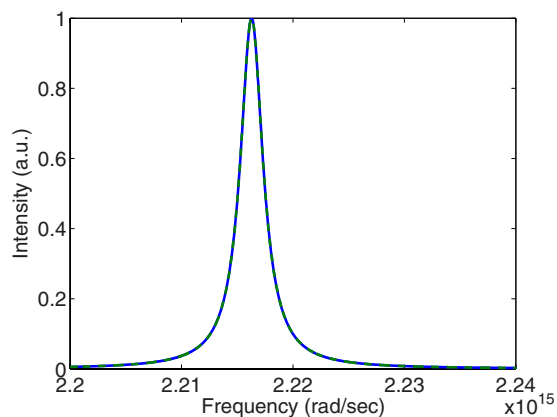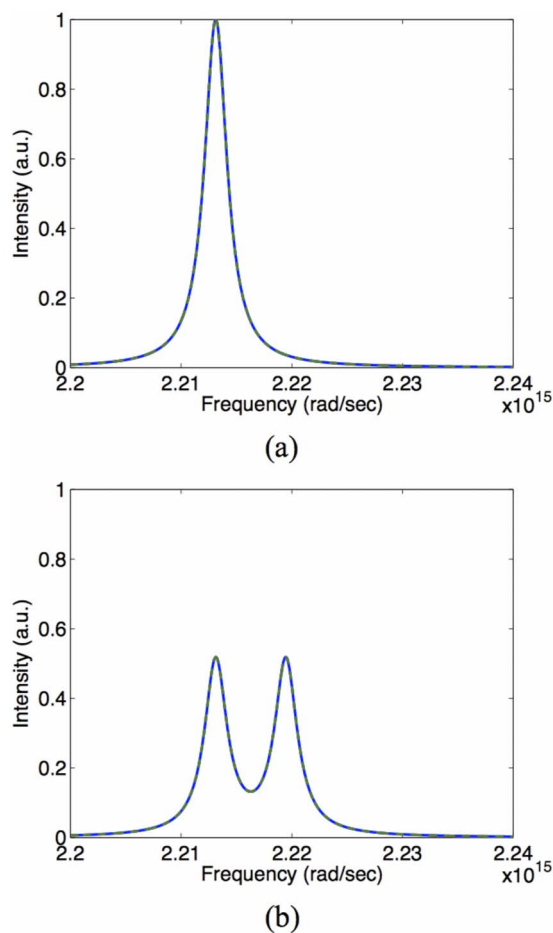

Fig. 2.   (Color online) Unperturbed power spectra for no detuning between the propagation constants of guides a and b. The spectra are identical.

both modes. This implies that one would expect both modes to turn on in a symmetric, coupled laser array (note that this analysis neglects mode competition, gain saturation, hole burning, etc., which would impose asymmetry in the array). In typical experiments, one mode is preferentially excited, and this mode usually dominates.

As mentioned above, the deterministic approach cannot predict partial spectral coherence regardless of the spectra or the coupling strength. However, this is not the case for stochastic boundary conditions, as is illustrated by Fig. 4. In this figure, the maximum spectral degree of coherence is plotted as a function of the coupling strength, κ. The frequency of maximum coherence changes with the value of κ, but it is typically at or near the resonances of the + and − modes. The plot shows that the maximum spectral degree of coherence increases as the coupling strength increases. This comes as a result of a decrease in the overlap between the line shapes of the two modes.

B. Asymmetric Coupled Guides
For the asymmetric calculations, the same definitions as in Table 3 are used except that $n_b = 3.495$. This example represents a two-element VCSEL array with some asymmetry between the array waveguides, such as a difference in aperture geometry or core index. Figure 5 shows the unperturbed spectra of the two uncoupled guides. As a result of the asymmetry, there is a noticeable splitting between the unperturbed resonances of the two guides.

The coupled spectra for deterministic boundary conditions are shown in Fig. 6. In this case, there is one mode that is dominant, again the + mode. However, it is apparent that there is some power in the − mode. This comes as a result of the detuning altering the + and − modes such that the boundary conditions excite an admixture of them. Despite this, the admixture represents a single coherent mode, and the spectral degree of coherence remains unity. Thus, the deterministic problem is shown to not allow for any partial spectral coherence between the fields of the two guides, even when more than one mode is present.

The random boundary conditions again provide an equal total excitation of the + and − modes as shown in Fig. 6. Now, however, the + mode is more localized in

Fig. 5. (Color online) Unperturbed power spectra for a small detuning between the propagation constants of guides a and b. The spectrum from a is shown with a solid curve, and the spectrum from b is shown with a dashed curve.

guide a, and the − mode is more present in guide b. Thus, random boundary conditions still cause both modes to turn on with equal total intensity, but the detuning serves to redistribute the modal power between the guides. In experiments, this redistribution of modal power can break

(a)

(b)

Fig. 6. (Color online) (a) Deterministic and (b) stochastic coupled power spectra for a small detuning between the propagation constants of guides a and b and $\kappa = 0.005$. The spectrum from a is shown with a solid curve, and the spectrum from b is shown with a dashed curve.
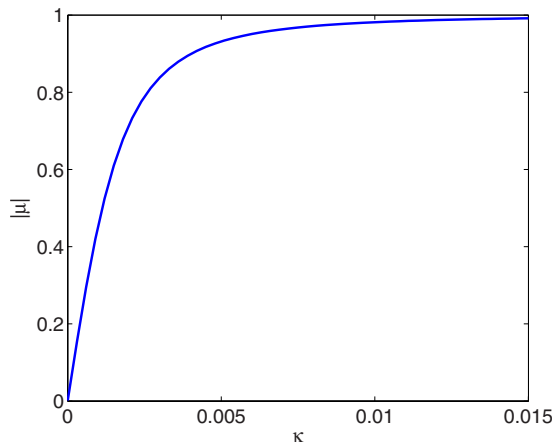

Fig. 4. (Color online) Maximum complex degree of coherence plotted as a function of the coupling strength κ for random boundary conditions and no detuning.
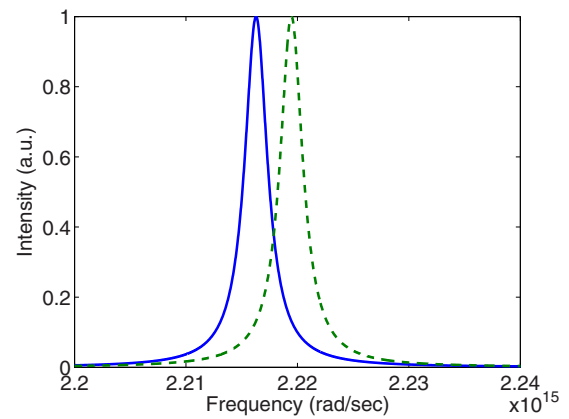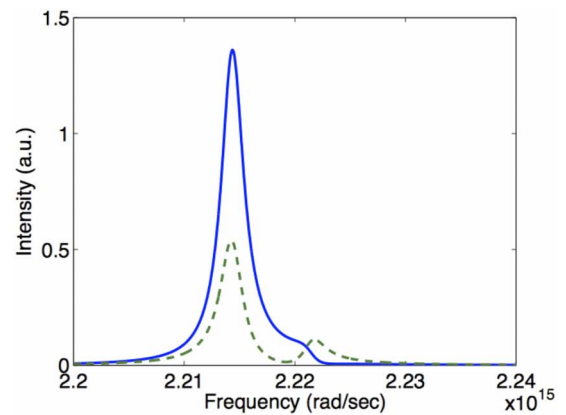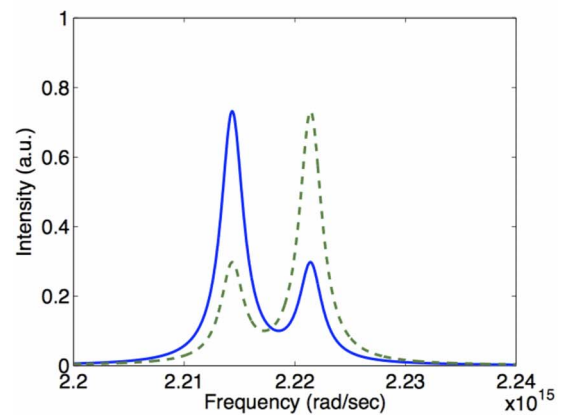
the symmetry that allows mode competition to select only one mode, and thus two incoherent modes can simultaneously lase.

Considering again the spectral degree of coherence for random boundary conditions, it is found that the trend is very similar to that seen in Fig. 4. The increase in coherence with κ is slightly slower with detuning, which suggests that the coupling strength has more influence on the degree of coherence than the detuning.

6. TIME-DOMAIN ANALYSIS OF STOCHASTIC COUPLED LASERS

A. Analytical Solutions
Real detectors provide a signal that is proportional to a time integral of the intensity falling on the detector. Therefore, the time-domain correlation functions are of primary importance. The time-domain correlation matrix is found by taking the Fourier transform of the frequency-domain matrix and is expressed as

$$\Gamma = \frac{1}{|2\eta|^2}\alpha\left(\frac{\pi}{2}\right)^{1/2}\begin{bmatrix}\Gamma_{aa} & \Gamma_{ab} \\ \Gamma_{ba} & \Gamma_{bb}\end{bmatrix}. \qquad (23)$$

In order to directly measure the time-domain cross correlations, let us assume that a pinhole is placed at the output facet over each waveguide such that the single-pinhole emissions are $\Gamma_{aa}(0)$ and $\Gamma_{bb}(0)$ from guides a and b, respectively. The far-field intensity produced by two pinholes is then (up to a multiplicative factor) [24]

$$I_{\text{FF}} = \Gamma_{aa}(0) + \Gamma_{bb}(0) + 2\Re\{\Gamma_{ab}(\tau)\}, \qquad (24)$$

where τ is the time offset between the signals from the two pinholes.

If the seeding fields are of equal intensity ($S_a^{(0)}=S_b^{(0)}=S^{(0)}$) and there is equal gain or loss in the two guides (Δn is real), the far field then becomes

$$I_{\text{FF}} = I_a^+ + I_b^+ + I_a^- + I_b^- + 2[I_a^+ I_b^+]^{1/2}e^{-\alpha|\tau|}\cos(\omega_+\tau + \phi)$$
$$- 2[I_a^- I_b^-]^{1/2}e^{-\alpha|\tau|}\cos(\omega_-\tau + \phi), \qquad (25)$$

where

$$I_a^+ = \sigma_+^2 S^{(0)}[(\eta - \Delta n)^2 + |\kappa|^2],$$

$$I_a^- = \sigma_-^2 S^{(0)}[(\eta + \Delta n)^2 + |\kappa|^2],$$

$$I_b^+ = \sigma_+^2 S^{(0)}[(\eta + \Delta n)^2 + |\kappa|^2],$$

$$I_b^- = \sigma_-^2 S^{(0)}[(\eta - \Delta n)^2 + |\kappa|^2]. \qquad (26)$$

In terms of the average frequency and the frequency difference

$$\bar{\omega} = \frac{\omega_- + \omega_+}{2},$$

$$\Delta\omega = \frac{\omega_- - \omega_+}{2}, \qquad (27)$$

and for sufficiently small $\Delta\omega\tau$ and $\alpha|\tau|$, Eq. (25) can be approximated as

$$I_{\text{FF}} \approx I_a^+ + I_b^+ + I_a^- + I_b^- + 2([I_a^+ I_b^+]^{1/2} - [I_a^- I_b^-]^{1/2})\cos(\bar{\omega}\tau + \phi). \qquad (28)$$

From this expression we can identify the temporal degree of coherence, γ, as defined in [24]

$$|\gamma| = \left|\frac{[I_a^+ I_b^+]^{1/2} - [I_a^- I_b^-]^{1/2}}{[(I_a^+ + I_a^-)(I_b^+ + I_b^-)]^{1/2}}\right|. \qquad (29)$$

The visibility of the far-field fringe pattern is

$$V = 2\frac{[I_a^+ I_b^+]^{1/2} - [I_a^- I_b^-]^{1/2}}{I_a^+ + I_b^+ + I_a^- + I_b^-}. \qquad (30)$$

Thus, using this analysis, it is possible to calculate the degree of coherence and visibility from the mode intensities in the two waveguides. Alternatively, partial coherence comes as a result of the existence of more than one coupled mode. It is proposed here that Eqs. (29) and (30) are general expressions that can be used to experimentally determine the degree of coherence of a laser array from measurement of the mode intensities present in the two guides. Note that, unlike in previous work [16], the visibility and degree of coherence are known exactly from the modal intensities, and a direct measure of the visibility is unnecessary. In other words, this theory directly predicts the visibility.

B. Numerical Analysis
Equations (29) and (30) describe the trends in visibility and degree of coherence with changing system parameters. To begin, let us consider a symmetric structure. The example of a VCSEL used in the previous numerical analyses is considered again here. For symmetric guides, the expressions for coherence and visibility reduce to identical forms. Therefore, it is sufficient to look at only the degree of coherence. Moreover, the degree of coherence can be found to be the same for any nonzero value of the coupling strength. Figure 7 shows the trend of degree of coherence with a changing ratio of spectral weightings. It can be seen here that the coherence monotonically decreases as the ratio of the modes approach unity.
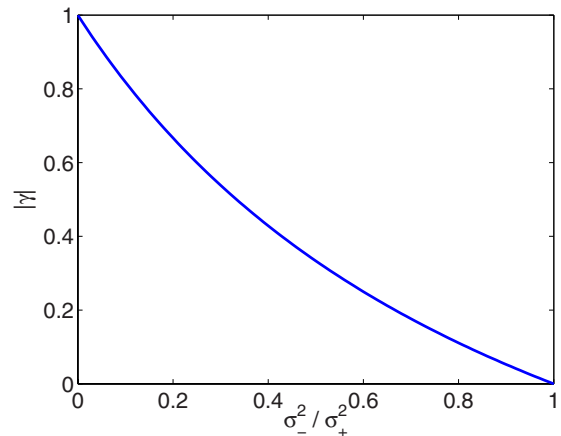

Fig. 7.   (Color online) Degree of coherence for symmetric coupled waveguides as a function of the ratio of the $-$ Mode spectral weighting to that of the $+$ mode.

As soon as there is some degree of detuning between the waveguides, the coupling strength has a significant influence. This can be seen in Fig. 8, where the degree of coherence is plotted for a detuning of $\Delta n = 0.005$ and coupling strengths $\kappa = 0.01$, $\kappa = 0.001$, and $\kappa = 0.0001$. It can be seen that stronger coupling tends to pull up the degree of coherence for intermediate ratios of the spectral weightings. This suggests that stronger coupling will tend to result in a higher degree of coherence even if two coupled modes are present.

As a result of the detuning, the visibility is no longer equal to the magnitude of the degree of coherence. Figure 8 illustrates the trends in visibility for the same conditions. It can be seen that the visibility is strongly influenced by the coupling strength. Moreover, with this detuning, the visibility never reaches unity as a result of the difference in intensities present in the two waveguides.

This analysis reveals that coupling strength plays a significant role in maintaining high coherence and visibility. In any practical laser array, some degree of asymmetry is present. If coupling is weak, the effects of the asymmetry will dominate, and low coherence will be observed.
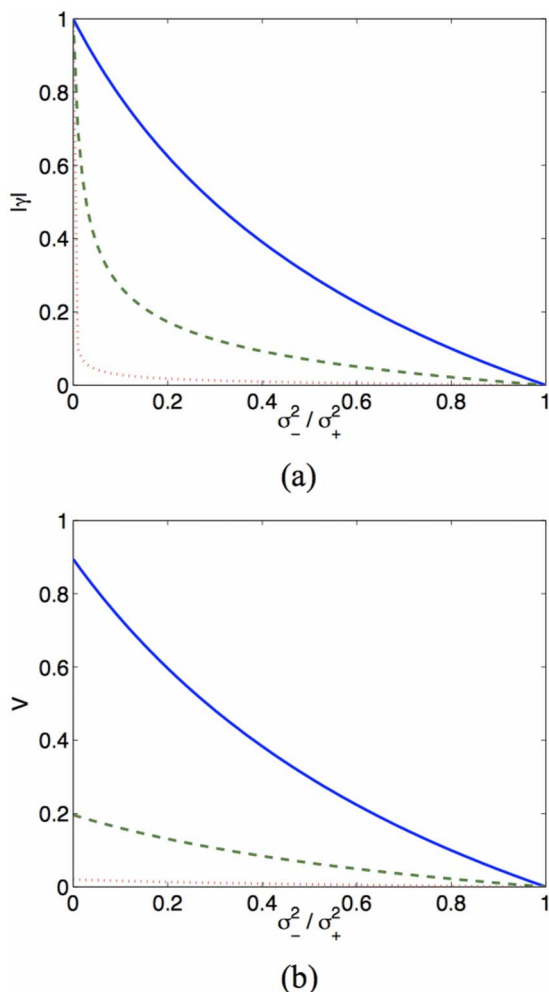
However, stronger coupling tends to counteract the asymmetry, and the degree of coherence increases with stronger coupling.

7. CONCLUSION

The coupled mode formalism with stochastic boundary conditions has been used to predict and investigate partial coherence in coupled semiconductor laser arrays. This model is an improvement over previous approaches as it is directly applicable to partially coherent coupled laser systems. In particular, the spectra and coupling can be calculated from the physical laser structure *ab initio*.

Calculations reveal that there is a strong connection between the spectral and temporal coherence and the number of coupled modes. For asymmetric systems (real devices are generally asymmetric to some degree), the degree of coherence scales with the coupling strength.

The approach presented here can be particularly useful for the design of single-mode coupled laser arrays. This work clearly demonstrates that more strongly coupled arrays are more likely to exhibit high coherence. Moreover, the formalism can be expanded to describe larger arrays without much increase in the complexity of the analysis. The future direction of this work will be to use this model to analyze and design coupled VCSEL arrays with a high degree of coherence.

Fig. 8.   (Color online) (a) Degree of coherence and (b) visibility for detuning $\Delta n = 0.005$ as a function of the ratio of the $-$ mode spectral weighting to that of the $+$ mode. The three curves are for coupling strengths $\kappa = 0.01$ (solid), $\kappa = 0.001$ (dashed), and $\kappa = 0.0001$ (dotted).

REFERENCES

1. H. Yoo, A. Scherer, J. Harbison, L. Florez, E. Paek, B. van der Gaag, J. Hayes, A. von Lehmen, E. Kapon, and Y. Kwon, "Fabrication of a two-dimensional phased array of vertical-cavity surface-emitting lasers," Appl. Phys. Lett. **56**, 1198–1200 (1990).
2. R. Morgan, K. Kojima, T. Mullally, G. Guth, M. Focht, R. Leibenguth, and M. Asom, "High-power coherently coupled 8×8 vertical cavity surface emitting laser array," Appl. Phys. Lett. **61**, 1160–1162 (1992).
3. M. Orenstein, E. Kapon, N. Stoffel, J. Harbison, L. Florez, and J. Wullert, "Two-dimensional phase locked arrays of vertical-cavity semiconductor lasers by mirror reflectivity modulation," Appl. Phys. Lett. **58**, 804–806 (1991).
4. L. Bao, N. Kim, L. Mawst, N. Elkin, V. Troshchieva, D. Vysotsky, and A. Napartovich, "Near-diffraction-limited coherent emission from large aperture antiguided vertical-cavity surface-emitting laser arrays," Appl. Phys. Lett. **84**, 320–322 (2004).
5. A. Lehman, D. Siriani, and K. Choquette, "Two-dimensional electronic beam-steering with implant-defined coherent vcsel arrays," Electron. Lett. **43**, 1202–1203 (2007).
6. P. Gourley, M. Warren, G. Hadley, G. Vawter, T. Brennan, and B. Hammons, "Coherent beams from high efficiency two-dimensional surface-emitting semiconductor laser arrays," Appl. Phys. Lett. **58**, 890–892 (1991).
7. F. Monti di Sopra, M. Brunner, H. Gauggel, H. Zappe, M. Moser, R. Hövel, and E. Kapon, "Continuous-wave operation of phase-coupled vertical-cavity surface-emitting laser arrays," Appl. Phys. Lett. **77**, 2283–2285 (2000).
8. A. Danner, J. Lee, J. Raftery, Jr, N. Yokouchi, and K. Choquette, "Coupled-defect photonic crystal vertical cavity surface emitting lasers," Electron. Lett. **39**, 1323–1324 (2003).
9. D. Serkland, K. Choquette, G. Hadley, K. Geib, and A. Allerman, "Two-element phased array of antiguided vertical-cavity lasers," Appl. Phys. Lett. **75**, 3754–3756 (1999).

10. D. Zhou and L. Mawst, "Two-dimensional phase-locked antiguided vertical-cavity surface-emitting laser arrays," Appl. Phys. Lett. **77**, 2307–2309 (2000).

11. K. Ebeling and L. Coldren, "Analysis of multielement semiconductor lasers," J. Appl. Phys. **54**, 2962–2969 (1983).

12. G. Hadley, "Modes of a two-dimensional phase-locked array of vertical-cavity surface-emitting lasers," Opt. Lett. **15**, 1215–1217 (1990).

13. T. Fishman, A. Hardy, and E. Kapon, "Formulations for calculating the eigenmodes of vertical-cavity laser arrays," IEEE J. Quantum Electron. **33**, 1756–1762 (1997).

14. J. Butler, D. Ackley, and D. Botez, "Coupled-mode analysis of phase-locked injection laser arrays," Appl. Phys. Lett. **44**, 293–295 (1984).

15. E. Kapon, J. Katz, and A. Yariv, "Supermode analysis of phase-locked arrays of semiconductor lasers," Opt. Lett. **9**, 125–127 (1984).

16. A. Lehman, J. Raftery, P. Carney, and K. Choquette, "Coherence of photonic crystal vertical-cavity surface-emitting laser arrays," IEEE J. Quantum Electron. **43**, 25–30 (2007).

17. A. C. Lehman Harren, K. D. Choquette, and P. S. Carney, "Partial coherence in coupled photonic crystal vertical cavity laser arrays," Opt. Lett. **34**, 905–907 (2009).

18. L. A. Coldren and E. R. Hegblom, *Vertical-Cavity Surface-Emitting Lasers: Design, Fabrication, and Applications* (Cambridge Univ. Press, 1999), Chap. 2, pp. 32–67.

19. S. L. Chuang, *Physics of Optoelectronic Devices* (Wiley, 1995).

20. R. Syms, "Simple approximate theory for twin-guide Fabry–Perot laser amplifier switches," J. Mod. Opt. **38**, 1167–1180 (1991).

21. A. Einstein, "Method for the determination of the statistical values of observations concerning quantities subject to irregular fluctuations," Arch. Sci. Phys. Nat. **37**, 254–256 (1914).

22. N. Wiener, "Generalized harmonic analysis," Acta Math. **55**, 117–258 (1930).

23. A. Y. Khintchine, "Correlation theory of stationary stochastic processes," Math. Ann. **109**, 604–615 (1934).

24. L. Mandel and E. Wolf, *Optical Coherence and Quantum Optics* (Cambridge Univ. Press, 1995).